





Original scientific paper

Electrochemical sensor for determination of hydroxylamine using functionalized Fe₃O₄ nanoparticles and graphene oxide modified screen-printed electrode

Hamed Tashakkorian^{1,2}, Behnaz Aflatoonian³, Peyman Mohammadzadeh Jahani⁴,
and Mohammad Reza Aflatoonian⁵,

¹Cellular and Molecular Biology Research Center (CMBRC), Health Research Institute, Babol University of Medical Sciences

²Department of Pharmacology, School of Medicine, Babol University of Medical Sciences, Babol, Iran

³Research Center of Tropical and Infectious Diseases, Kerman University of Medical Sciences, Kerman, Iran

⁴School of Public Health, Bam University of Medical Sciences, Bam, Iran

⁵Leishmaniasis Research Center, Kerman University of Medical Sciences, Kerman, Iran

Corresponding author: ✉ peyman1234@gmail.com; ✉ m.aflatoonian97@gmail.com

Received: October 19, 2021; Accepted: November 2, 2021; Published: November 17, 2021

Abstract

A simple strategy for determination of hydroxylamine based on Fe₃O₄ nanoparticles functionalized by [2-(4-((3-(trimethoxysilyl)propylthio)methyl)-1H-1,2,3-triazol-1-yl)acetic acid] (FNPs) and graphene oxide (GO) modified screen-printed electrode (SPE), denoted as (Fe₃O₄ FNPs/GO/SPE), is reported. The electrochemical behavior of hydroxylamine was investigated at Fe₃O₄FNPs/GO/SPE by cyclic voltammetry (CV), differential pulse voltammetry (DPV) and chronoamperometry (CHA) techniques in phosphate buffer solution (pH 7.0). Fe₃O₄ FNPs/GO/SPE as a novel electrochemical sensor exhibited catalytic activity toward the oxidation of hydroxylamine. The potential of hydroxylamine oxidation was shifted to more negative potentials, and its oxidation peak current increased on the modified electrode, also indicating that under these conditions, the electrochemical process is irreversible. The electrocatalytic current of hydroxylamine showed a good relationship in the concentration range of 0.05–700.0 μM, with a detection limit of 10.0 nM. The proposed electrode was applied for the determination of hydroxylamine in water samples, too.

Keywords

hydroxylamine; electroanalysis; voltammetry; modified electrode;

Introduction

Hydroxylamine is one of the important compounds in the chemical industry. Hydroxylamine, a derivative of ammonia is one of the reducing agents widely used in industry and pharmacy. It is

identified as a key intermediate in the nitrogen cycles and production of nitrous oxide [1]. Hydroxylamine is a well-known mutagen, which induces highly specific mutations with the nucleic acid cytosine. Modest levels of hydroxylamine can be toxic to humans, animals and even plants [2]. Also, in the industry, it can be used as a raw material for the synthesis of pharmaceutical intermediates and final drug substances. Therefore, from the industrial, environmental and health viewpoints, the development of a sensitive analytical method for the determination of hydroxylamine is very important [3-5].

Due to the simple sample preparation, low-cost instrumentation, high sensitivity, selectivity, accuracy and precision of electrochemical methods, they have been used widely in biological and environmental analysis. However, many analytes exhibit irreversible oxidation requiring large overpotential at conventional electrodes [6-10]. Therefore, the use of chemically modified electrodes for the analysis of metals and organics is a well-established practice [11-14].

A conductive substrate modified with electroactive thin films, monolayers, or thick coatings results in a chemically modified electrode. The modification of the conductive substrate has positive effects on (i) electron transfer kinetics, (ii) electrocatalytic activity due to the use of materials with large surface area, (iii) sensitivity of measurement in electroanalytical applications, (iv) selectivity toward specific molecules due to immobilized functional groups, and (v) extraction and accumulation of an analyte at the electrode surface [15,16]. Researchers have recently focused on designing and synthesizing nano-materials for various applications due to their unique physical and chemical properties [17-21]. Nano-materials as modifiers are used in various sensor and biosensor applications because they exhibit good electrocatalytic properties, high stability, high surface-to-volume ratio, and wide availability and provide fast electron transfer rates. Metal nanoparticles, which exhibit very interesting physico-chemical properties, are among the materials most commonly used for the modification of electrodes. In recent years, magnetic nanoparticles of iron oxide (Fe_3O_4) have attracted considerable interest due to their particular attributes, such as magnetic and optical properties, low toxicity, biocompatibility and easy preparation. Many of the electrical and magnetic properties of metal nanoparticles are attributed to the electron transfer between Fe^{2+} and Fe^{3+} centers present in the oxide chemical structure [22,23]. Graphene oxide (GO) is a compound with different ratios of carbon, oxygen, and hydrogen, which is a derivative of graphene. The presence of various functional groups such as epoxy, hydroxy and carboxyl on the GO surface affects the oxidation degree of graphene oxide [24]. The unique physicochemical properties such as large specific surface area and high conductivity suggest a great potential for GO to provide new approaches and critical improvements in the field of electrochemistry [25].

According to the previous points, it is important to create suitable conditions for the analysis of hydroxylamine. In this study, we describe the application of functionalized Fe_3O_4 nanoparticles as a nanostructure sensor for the voltammetric determination of hydroxylamine. Eventually, the analytical performance of the suggested sensor for hydroxylamine determination in water samples is evaluated.

Experimental

Instrumentation

An Autolab PGSTAT 302N instrument (Eco Chemie, The Netherlands) and a general-purpose electrochemical system software were used to perform and control the experiments. The screen-printed electrode (DropSens, DRP-110, Spain, working: 4 mm diameter) consists of three main parts: graphite counter electrode, silver pseudo-reference electrode, and graphite working electrode. pH

measurements were performed using a Metrohm 710 pH-meter. Field emission scanning electron microscopy (FESEM) was recorded on a Hitachi S4160 instrument (Tokyo, Japan).

Reagents

Analytical grade reagents were obtained from Merck Co. (Darmstadt, Germany). Orthophosphoric acid buffer solutions ($2.0 < \text{pH} < 12.0$) were prepared using the acid and its salts (KH_2PO_4 , K_2HPO_4 , and K_3PO_4). All solutions were freshly prepared using double distilled water.

Synthesis of Fe_3O_4 FNPs

The modified 2-(4-((3-(trimethoxysilyl) propylthio)methyl)-1H-1,2,3-triazol-1-yl)acetic acid- Fe_3O_4 nanoparticles (Fe_3O_4 FNPs) were prepared in the following four-step procedure:

Step 1

In a round-bottomed flask, propargyl bromide (0.11 mL, 1mmole) was added to the mixture of 15 ml acetone containing 3-mercaptopropyl(trimethoxy)silane (0.195 mL, 1.05 mmol) and potassium carbonate (0.167 g, 1.2 mmol). The reaction medium was kept for 20 hours in this condition at 70 °C while being stirred under N_2 . After the specified time, the reaction mixture was filtered, and the solvent was evaporated with a rotary evaporator. The product was obtained by two-phase ethylacetate/water) extraction procedure, and washed with 5 % NaHCO_3 and brine solution, giving oily trimethoxy(3-(prop-2-yn-1-ylthio)propyl)silane. The oily product can be incorporated in the next step (step 2) without any further purification. Analytical calculation for $\text{C}_9\text{H}_{18}\text{O}_3\text{SSi}$ gave: C: 46.15 %, H: 7.69 %, S: 13.67 %; elemental analysis found: C:46.46 %; H:7.25 %, S: 13.38 %.

Step 2

To the solution of chloroacetic acid (0.094 g, 1 mmol) in 15 mL DMF, sodium azide (0.072 g, 1.05 mmol) was added, and the mixture was stirred at 90 °C for 24 hours. Then the solution was kept for the next step of the synthesis.

Step 3

This compound was synthesized based on click protocol and the preparation of triazole compounds discussed in our previous articles [26,27] thoroughly. One-pot synthesis of compound 3 was carried out by the addition of trimethoxy(3-(prop-2-yn-1-ylthio)propyl)silane (1) (1 mmol) to a freshly prepared 15 DMF solution of 2-azidoacetic acid. Then, $\text{CuSO}_4 \cdot 5\text{H}_2\text{O}$ (0.075 g, 0.3 mmol), sodium ascorbate (0.346 g, 1.5 mmol) and 2 ml of water were added to the reaction mixture. The mixture was stirred at room temperature for 30 hours. After the appropriate time, the mixture was poured into the water (30 ml) to remove the unwanted compounds. The product was extracted with 25 ml of ethyl acetate and washed with 1M ammonium hydroxide (15 ml) for removing the unreacted copper ions. The organic phase was washed for another time and dried over MgSO_4 . After filtration, the solvent was removed under reduced pressure by Heidolph rotary evaporator to obtain the oily product 3. Analytical calculation for $\text{C}_{11}\text{H}_{21}\text{N}_3\text{O}_5\text{SSi}$ gave: C: 39.40 %, H: 6.27 %, N: 12.54 %, S: 9.55 %; Elemental analysis found: C: 39.76 %; H: 5.95 %, N: 12.34 %, S: 9.28 %.

Step 4

$\text{FeCl}_3 \cdot 6\text{H}_2\text{O}$ (1.9 g) and $\text{FeCl}_2 \cdot 4\text{H}_2\text{O}$ (0.67 g) were dissolved in 50 ml of deionized water under an argon atmosphere [28]. After half an hour, 3 mL of ammonium hydroxide solution (25 %) was added to the solution and the pH value was maintained around 11 with continuous stirring using a magnetic stirrer. After the addition of the mentioned volume of the ammonia solution, a deep black magnetite

precipitate was formed immediately. Stirring was continued for another 1 hour under an argon atmosphere. The resulting precipitate was collected using a magnet and washed several times with deionized water to remove the excess amount of ammonia and until the pH of eluent water became neutral. The magnetite nanoparticles were kept in the dark glass for further applications.

In a 50 ml round-bottomed flask, 1 g of magnetic nanoparticles (Fe_3O_4) was added to the solution of the synthesized compound 3 in DMF (30 ml). The reaction mixture was sonicated for 10 minutes using an ultrasonic bath and heated at 110 °C for 24 hours under an argon atmosphere to reach the maximum dispersion. After the specified time, the functionalized magnetic nanoparticles were collected using a magnet and washed with DMF and acetone, respectively. The precipitate was kept in the dark glass and stored in a desiccator.

The FESEM image of magnetic nanoparticles is displayed in Figure 1.

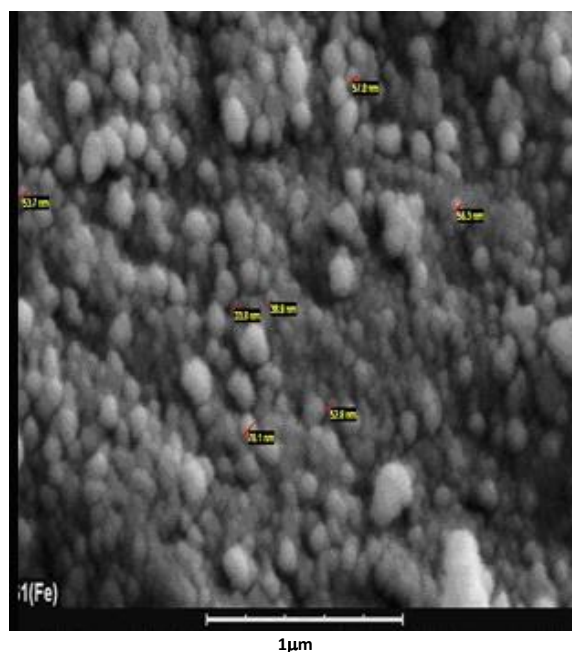


Figure 1. FESEM of $\text{Fe}_3\text{O}_4\text{F}$ NPs derivative

Preparation of Fe_3O_4 FNP/GO/SPE

The bare screen-printed electrode was coated with functionalized Fe_3O_4 nanoparticles (Fe_3O_4 FNPs) and GO as follows: a stock solution of Fe_3O_4 FNPs and GO in 1 mL aqueous solution was prepared by dispersing 1 mg Fe_3O_4 FNPs and 1 mg GO with ultrasonication for 1 h. Then, 5 μl aliquot of Fe_3O_4 FNPs-GO/ H_2O suspension solution was cast on the carbon working electrodes and waited until the solvent was evaporated at room temperature.

The surface area of Fe_3O_4 FNP/GO/SPE and bare SPE were obtained by CV using 1 mM $\text{K}_3\text{Fe}(\text{CN})_6$ at different scan rates. Using the Randles-Sevcik formula [29] for Fe_3O_4 FNP/GO/SPE, the electrode surface was 0.081 cm^2 which was about 2.6 times greater than bare SPE.

Result and discussion

Electrochemical profile of hydroxylamine on Fe_3O_4 FNP/GO/SPE

Since the electrochemical behaviour of hydroxylamine is pH-dependent, the optimizing pH of the solution is necessary for obtaining the best results. Hence, the evaluations were performed at different pH values ranging from 2.0–9.0. Results presented in Figure 2 showed that the best result during the electro-oxidation of hydroxylamine at the surface of the modified electrode is obtained at pH 7.0.

Figure 3 illustrates the cyclic voltammograms of 200.0 μM hydroxylamine in 0.1 M PBS at Fe_3O_4 FNP/GO/SPE (curve a) and unmodified SPE (curve b). As it can be easily noticed, the maximum oxidation of hydroxylamine occurs at 860 mV in the case of Fe_3O_4 FNP/GO/SPE, which is around 165 mV more negative than observed in the case of unmodified SPE.

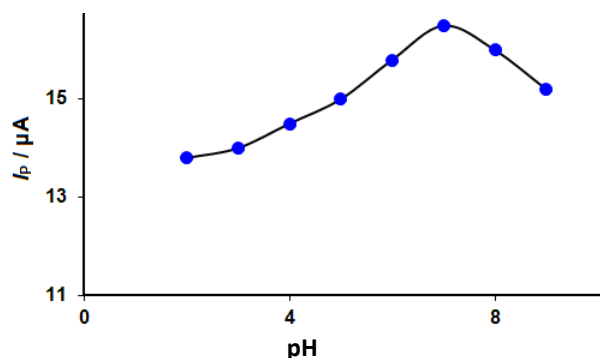


Figure 2. Plot of I_p vs. pH obtained from DPVs of Fe_3O_4 FNP/GO/SPE in a solution containing 200.0 μM of hydroxylamine in 0.1 M PBS of different pH (2.0, 3.0, 4.0, 5.0, 6.0, 7.0, 8.0 and 9.0)

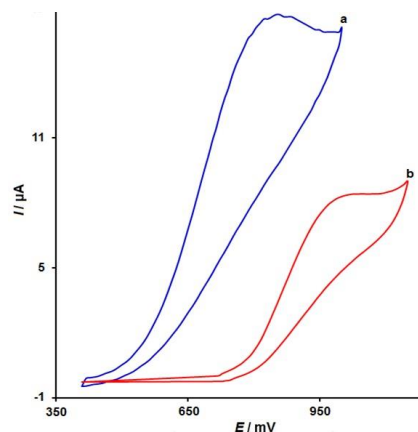


Figure 3. Cyclic voltammograms of (a) Fe_3O_4 FNP/GO/SPE and (b) bare SPE in 0.1 M PBS (pH 7.0) in the presence of 200.0 μM hydroxylamine at the scan rate 50 mV s^{-1}

Effect of scan rate

Figure 4 illustrates the effects of potential scan rates on the oxidation currents of hydroxylamine, indicating that increasing the scan rate increased the peak currents. Also, based on the fact that the plot of I_p against the square root of the potential scan rate ($v^{1/2}$) is linear (cf. inset of Figure 4), it was concluded that the oxidation process of hydroxylamine at Fe_3O_4 FNP/GO/SPE is diffusion controlled.

Further, the Tafel curve of hydroxylamine was plotted using data from the rising sections of the current-voltage curves (*i.e.*, Tafel regions) obtained at 10 mV s^{-1} (Figure 5).

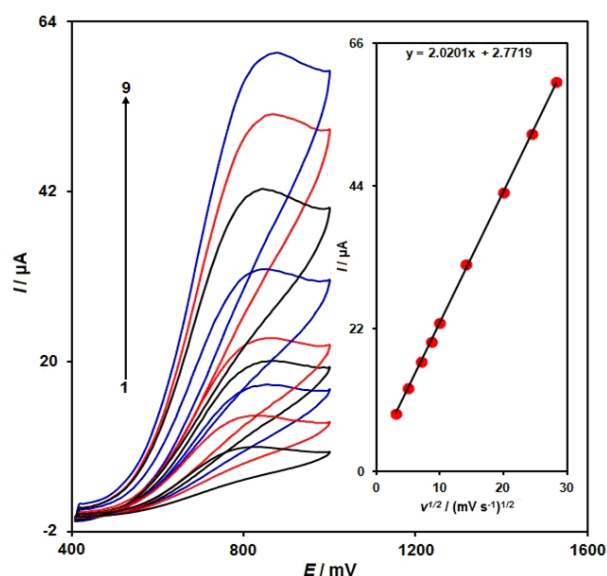


Figure 4. Cyclic voltammograms of Fe_3O_4 FNP/GO/SPE in 0.1 M PBS (pH 7.0) containing 200.0 μM hydroxylamine at various scan rates. 1-9 correspond to 10, 25, 50, 75, 100, 200, 400, 600 and 800 mV s^{-1} . Inset: variation of anodic peak current vs. $v^{1/2}$

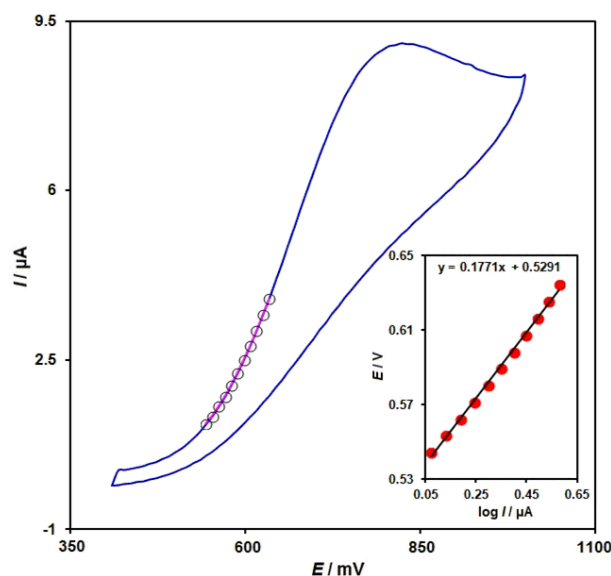


Figure 5. Cyclic voltammogram (10 mV s^{-1}) of electrode in 0.1 M PBS (pH 7.0) containing 200.0 μM hydroxylamine. The points are data used for the Tafel plot shown in the inset

The Tafel region of the current-potential curve is influenced by the electron transfer kinetics of the electrode reactions. The results showed a Tafel slope of 0.1771 V, indicating one-electron transfer as the rate-determining step for the electrode process [24] for charge transfer coefficient (α) of 0.67.

Chronoamperometric analysis

The chronoamperometric analysis of hydroxylamine using Fe₃O₄FNPs/GO/SPE was performed at 0.92 V vs. Ag/AgCl/KCl (3.0 M) and the results were obtained for different hydroxylamine samples in PBS (pH 7.0) are illustrated in Figure 6.

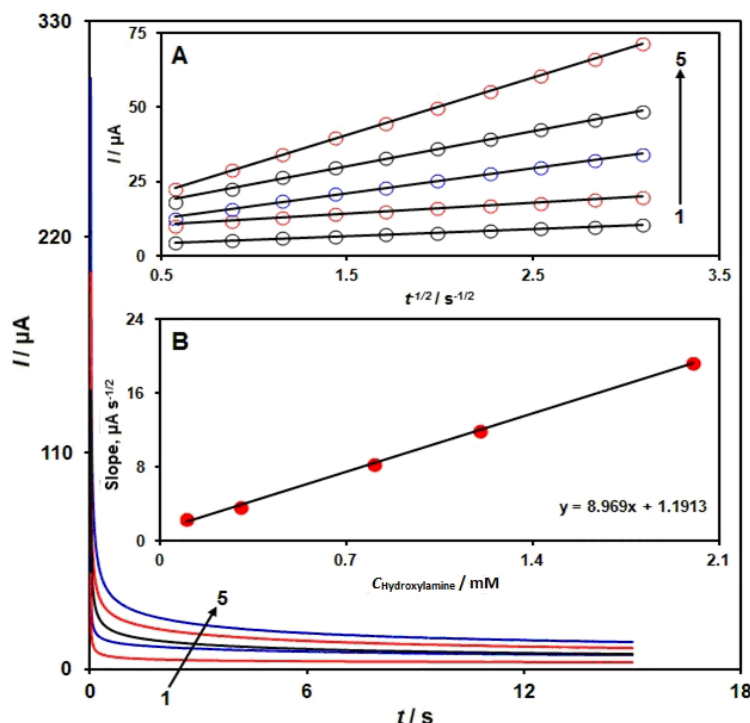


Figure 6. Chronoamperograms obtained at Fe₃O₄FNPs/GO/SPE in 0.1 M PBS (pH 7.0) for different concentrations of hydroxylamine (1–5 correspond to 0.1, 0.3, 0.8, 1.2 and 2.0 mM). Insets: (A) plots of I vs. $t^{-1/2}$ obtained from chronoamperograms 1–5; (B) the plot of the slope of the straight lines against hydroxylamine concentration

For chronoamperometric analysis of electroactive materials under mass transfer limited conditions, the Cottrell equation [29] can be applied. Cottrell equation is defined as:

$$I = nFAD^{1/2}C_b\pi^{-1/2}t^{-1/2}$$

where D is the diffusion coefficient, and C_b is the bulk concentration (mol cm^{-3}), A is the geometric area of the electrode, n is the number of electrons, F is the Faraday number, and t is the time. Experimental plots of I vs. $t^{-1/2}$ were employed, with the best fits for different concentrations of hydroxylamine shown in Figure 6A. The slopes of the resulting straight lines were then plotted vs. hydroxylamine concentration (Figure 6B). From the resulting slope and Cottrell equation, the mean value of D for hydroxylamine was found to be $6.86 \times 10^{-6} \text{ cm}^2 \text{ s}^{-1}$.

Calibration curve and limit of detection

The peak currents obtained for hydroxylamine using Fe₃O₄FNPs/GO/SPE were utilized for the quantitative analysis of hydroxylamine in water solutions. Given the advantage of differential pulse voltammetry (DPV) in terms of improved sensitivity and better characteristics for analytical applications, the modified electrode was used as the working electrode in DPV analyses in a range of hydroxylamine

solutions in 0.1 M PBS. DPV (step potential=0.01 V and pulse amplitude = 0.025 V) results presented in Figure 7 show a linear relationship between the peak currents and concentrations of hydroxylamine over the concentration range of 0.05-700.0 μM . The correlation coefficient of 0.9987 and-detection limit (3σ) of 10.0 ± 0.02 nM was obtained.

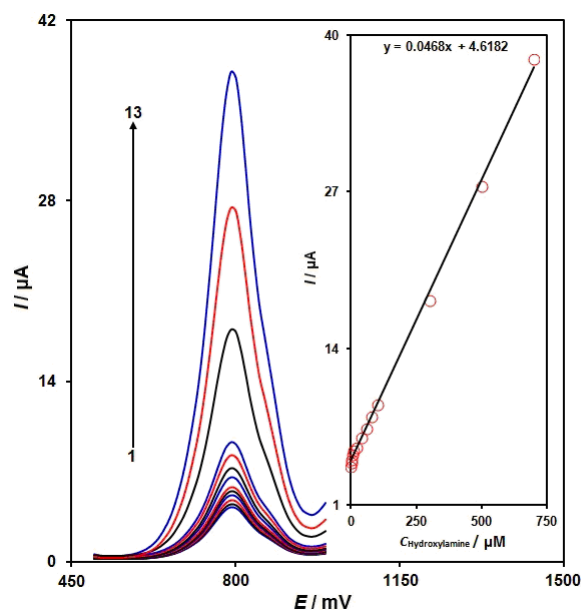


Figure 7. DPVs of Fe_3O_4 FNPs/GO/SPE in 0.1 M (pH 7.0) containing different concentrations of hydroxylamine (1–13 correspond to 0.05, 0.25, 1.0, 5.0, 10.0, 20.0, 40.0, 60.0, 80.0, 100.0, 300.0, 500.0 and 700.0 μM). Inset: plot of oxidation peak current as a function of hydroxylamine concentration in the range of 0.05-700.0 μM

Analysis of real samples

To assess the applicability of the modified electrode for the determination of hydroxylamine in real samples by using DPV, the described method was applied to the determination of hydroxylamine in tap, river and well water samples. The standard addition method was used for this analysis, and the results are given in Table 1. The observed recovery of hydroxylamine was satisfactory, and the reproducibility of the results was demonstrated based on the mean relative standard deviation (RSD).

Table 1. The application of Fe_3O_4 FNP/SPE for determination of hydroxylamine in water samples ($n=5$)

Sample	Concentration, μM		Recovery, %	RSD, %
	Spiked,	Found, μM		
Tap water	0	ND	-	-
	5.0	4.9	98.0	2.4
	10.0	10.2	102.0	3.3
	15.0	15.5	103.3	2.7
	20.0	19.8	99.0	2.1
River water	0	ND	-	-
	7.5	7.7	102.7	1.9
	12.5	12.4	99.2	2.8
	17.5	17.8	101.7	2.4
	22.5	23.2	103.1	3.2
Well water	0	ND	-	-
	10.0	9.8	98.0	3.4
	20.0	19.8	99.0	1.8
	30.0	30.7	102.3	2.7
	40.0	39.5	98.7	2.4

Conclusion

We have demonstrated the highly sensitive electrochemical determination of hydroxylamine using Fe₃O₄FNPs and GO modified SPE. Fe₃O₄FNPs/GO/SPE showed two times higher oxidation current with 165 mV less positive potential shift for hydroxylamine compared to bare SPE. The current response was increased linearly while increasing the concentration of hydroxylamine from 0.05 to 700.0 μM and a detection limit was found to be 10.0 nM (*S/N* = 3). The practical application of the present modified electrode was demonstrated by measuring the concentration of hydroxylamine in water samples.

References

- [1] S. Liu, H. Vereecken, N. Brüggemann, *Geoderma* **232** (2014) 117-122. <https://doi.org/10.1016/j.geoderma.2014.05.006>
- [2] C. Zhao, J. Song, *Analytica Chimica Acta* **434** (2001) 261-267. [https://doi.org/10.1016/S0003-2670\(01\)00846-7](https://doi.org/10.1016/S0003-2670(01)00846-7)
- [3] J. P. Guzowski Jr, C. Golanoski, E. R. Montgomery, *Journal of Pharmaceutical and Biomedical Analysis* **33** (2003) 963-974. [https://doi.org/10.1016/S0731-7085\(03\)00433-3](https://doi.org/10.1016/S0731-7085(03)00433-3)
- [4] M. P. Ngoc Bui, X. H. Pham, K. N. Han, C. A. Li, E. K. Lee, H. J. Chang, G. H. Seong, *Electrochemistry Communications* **12** (2010) 250-253. <https://doi.org/10.1016/j.elecom.2009.12.006>
- [5] P. N. Fernando, I. N. Egwu, M. S. Hussain, *Journal of Chromatography A* **956** (2002) 261-270. [https://doi.org/10.1016/S0021-9673\(02\)00145-0](https://doi.org/10.1016/S0021-9673(02)00145-0)
- [6] A. Hosseini Fakhrabad, R. Sanavi Khoshnood, M. R. Abedi, M. Ebrahimi, *Eurasian Chemical Communications* **3** (2021) 627-634. <http://dx.doi.org/10.22034/ecc.2021.288271.1182>
- [7] R. Rajaram, J. Mathiyarasu, *Colloids and Surfaces B* **170** (2018) 109-114. <https://doi.org/10.1016/j.colsurfb.2018.05.066>
- [8] P. Prasad, N.Y. Sreedhar, *Chemical Methodologies* **2** (2018) 277-290. <https://doi.org/10.22034/CHEMM.2018.63835>
- [9] S. Azimi, M. Amiri, H. Imanzadeh, A. Bezaatpour, *Advanced Journal of Chemistry A* **4** (2021) 152-164. <https://doi.org/10.22034/ajca.2021.275901.1246>
- [10] J. Wang, J. Yang, P. Xu, H. Liu, L. Zhang, S. Zhang, L. Tian, *Sensors and Actuators B: Chemical* **306** (2020) 127590. <https://doi.org/10.1016/j.snb.2019.127590>
- [11] F. Mehri-Talarposhti, A. Ghorbani-Hasan Saraei, L. Golestan, S.A. Shahidi, *Asian Journal of Nanosciences and Materials* **3** (2020) 313-320. <https://doi.org/10.26655/AJNANOMAT.2020.4.5>
- [12] E. Naghian, E. M. Khosrowshahi, E. Sohoul, F. Ahmadi, M. Rahimi-Nasrabadi, V. Safarifard, *New Journal of Chemistry* **44** (2020) 9271-9277. <https://doi.org/10.1039/D0NJ01322F>
- [13] M. Pirozmand, A. Nezhadali, M. Payehghadr, L. Saghatforoush. *Eurasian Chemical Communications* **2** (2020) 1021-1032. <https://doi.org/10.22034/ECC.2020.241560.1063>
- [14] L. Han, H. Tao, M. Huang, Y. Zhang, S. Qiao, R. Shi, *Russian Journal of Electrochemistry* **52** (2016) 115-122. <https://doi.org/10.1134/S1023193516020051>
- [15] J. Yi, S. Tang, Z. Wang, Y. Yin, S. Yang, B. Zhang, S. Shu, T. Liu, L. Xu, *International Journal of Environmental Analytical Chemistry* **95** (2015) 158-174. <https://doi.org/10.1080/03067319.2014.994616>
- [16] X. C. Lu, L. Song, T. T. Ding, Y.L. Lin, C. X. Xu, *Russian Journal of Electrochemistry* **53** (2017) 366-373. <https://doi.org/10.1134/S1023193517040073>
- [17] S. S. Mahmood, A. J. Atiya, F. H. Abdulrazzak, A. F. Alkaim, F. H. Hussein, *Journal of Medicinal and Chemical Sciences* **4** (2021) 225-229. <https://doi.org/10.26655/JMCHEMSCI.2021.3.2>
- [18] S. Saeidi, F. Javadian, Z. Sepehri, Z. Shahi, F. Mousavi, M. Anbari, *International Journal of Advanced Biological and Biomedical Research* **4** (2016) 96-99. <http://dx.doi.org/10.26655/ijabbr.2016.2.12>

- [19] R. Jabbari, N. Ghasemi, *Chemical Methodologies* **5** (2021) 21-29. <https://doi.org/10.22034/chemm.2021.118446>
- [20] A. G. El-Shamy, *Materials Chemistry and Physics* **243** (2020) 122640. <https://doi.org/10.1016/j.matchemphys.2020.122640>
- [21] S. Gupta, M. Lakshman, *Journal of Medicinal and Chemical Sciences* **2** (2019) 51-54. <https://doi.org/10.26655/JMCHEMSCI.2019.3.3>
- [22] C. P. Sousa, R. C. de Oliveira, T. M. Freire, P. B. A. Fechine, M. A. Salvador, P. Homem-de-Mello, S. Morais, P. de Lima-Neto, A. N. Correia, *Sensors and Actuators B: Chemical* **240** (2017) 417-425. <https://doi.org/10.1016/j.snb.2016.08.181>
- [23] M. P. Kingsley, P. B. Desai, A. K. Srivastava, *Journal of Electroanalytical Chemistry* **741** (2015) 71-79. <https://doi.org/10.1016/j.jelechem.2014.12.039>
- [24] F. Li, X. Jiang, J. Zhao, S. Zhang, *Nano Energy* **16** (2015) 488–515. <https://doi.org/10.1016/j.nanoen.2015.07.014>
- [25] N. N. Song, Y. Z. Wang, X. Y. Yang, H. L. Zong, Y. X. Chen, Z. Ma, C. X. Chen, *Journal of Electroanalytical Chemistry* **873** (2020) 114352. <https://doi.org/10.1016/j.jelechem.2020.114352>
- [26] M. M. Lakouraj, H. Tashakkorian, *Supramolecular Chemistry* **25** (2013) 221-232. <https://doi.org/10.1080/10610278.2012.758366>
- [27] M. M. Lakouraj, H. Tashakkorian, *Journal of Macromolecular Science, Part A*, **50** (2013) 310-320. <https://doi.org/10.1080/10601325.2013.755859>
- [28] M. S. Darwish, N. H. Nguyen, A. Ševcū, I. Stibor, *Journal of Nanomaterials* **16** (2015) 89. <https://doi.org/10.1155/2015/416012>
- [29] A. J. Bard, L. R. Faulkner, *Electrochemical Methods Fundamentals and Applications, second ed*, Wiley, New York, 2001.

